ChemPubSoc Europe

DOI: 10.1002/chem.201400179

CHEMISTRY A European Journal Full Paper

Hydrogen Bonds

Halometallate Complexes of Germanium(II) and (IV): Probing the Role of Cation, Oxidation State and Halide on the Structural and Electrochemical Properties

Philip N. Bartlett, Charles Y. Cummings, William Levason, David Pugh, and Gillian Reid*[a]

Abstract: The Ge^{IV} chlorometallate complexes, $[EMIM]_2[GeCl_6]$, $[EDMIM]_2[GeCl_6]$ and $[PYRR]_2[GeCl_6]$ (EMIM = 1-ethyl-3-methylimidazolium; EDMIM = 2,3-dimethyl-1-ethylimidazolium; PYRR = *N*-butyl-*N*-methylpyrrolidinium) have been synthesised and fully characterised; the first two also by single-crystal X-ray diffraction. The imidazolium chlorometallates exhibited significant C–H···Cl hydrogen bonds, resulting in extended supramolecular assemblies in the solid state. Solution ^1H NMR data also showed cation–anion association. The synthesis and characterisation of Ge^{II} halometallate salts $[EMIM][GeX_3]$ (X = Cl, Br, I) and $[PYRR][GeCl_3]$, including single-crystal X-ray analyses for the homologous series of imidazolium salts, are reported. In these complexes, the intermolecular interactions are much weaker in the solid state and they appear not to be significantly associated in solution. Cyclic-voltammetry experiments on the Ge^{IV} species in CH_2Cl_2 solution showed two distinct, irreversible reduction waves attributed to Ge^{IV}–Ge^{II} and Ge^{II}–Ge^0, whereas the Ge^{II} species exhibited one irreversible reduction wave. The potential for the Ge^{II}–Ge^0 reduction was unaffected by changing the cation, although altering the oxidation state of the precursor from Ge^{IV} to Ge^{II} does have an effect; for a given cation, reduction from the $[GeCl_3]^-$ salts occurred at a less cathodic potential. The nature of the halide co-ligand also has a marked influence on the reduction potential for the Ge^{II}–Ge^0 couple, such that the reduction potentials for the $[GeX_3]^-$ salts become significantly less cathodic when the halide (X) is changed Cl→Br→I.

Introduction

Germanium is a highly important element with applications ranging from microelectronics to photovoltaics.[1] Its large Bohr exciton radius (24.3 nm) means it is a leading candidate to replace silicon for quantum computing applications.[2] Industrially, films of germanium are deposited by vapour-phase epitaxy from GeH_4, although there is a drive to find alternative precursors and/or alternative deposition techniques to avoid the use of toxic and flammable GeH_4.[3]

Electrodeposition is one alternative technique. Conventional aqueous electrodeposition of germanium is difficult, because a very negative cathodic potential is required for the reduction of Ge^{IV} to elemental germanium. Water, with a narrow potential window, is generally considered unsuitable as a solvent, although there are a few instances of its use in Ge electrodeposition. Maldonado and co-workers have used a basic solution of GeO_2 in the presence of a liquid Hg electrode, forming a supersaturated Ge amalgam in situ, from which crystalline Ge was obtained.[4] Stickney and co-workers have also used aqueous basic GeO_2 to obtain electrodeposited Ge. Initial attempts suffered from poor film thickness (3.5 monolayers on Au) and alloying between Ge and Au.[5] However, by electrodepositing a monolayer of Te on a Cu electrode before introducing the Ge precursor solution, a 50 nm film of Ge could be obtained with concomitant stripping of the Te monolayer.[6]

Germanium electrochemistry is challenging due to the sensitivity of many Ge-containing precursors (such as $GeCl_4$) towards trace amounts of water, for example, residual water in solvents such as acetonitrile. Various coordination compounds of germanium have been studied electrochemically;[7] however, the electrochemistry has typically contained contributions from the ligands, as well as the germanium centre. Nonetheless, in recent years, there have been several studies detailing both the electrochemistry of the germanium centre and the electrodeposition of germanium to form thin films. In particular, Endres' group has investigated GeX_4 (X = Cl, Br, I)[8] in room-temperature ionic liquids (RTILs), such as $[BMIM][PF_6]$ and $[PYRR][NTf_2]$ (BMIM = 1-butyl-3-methylimidazolium; PYRR = N-butyl-*N*-methylpyrrolidinium; Tf = trifluoromethanesulfonyl, Figure 1).[9] These RTILs have wide potential windows and are highly conductive. However, they can be difficult to purify and impurities (often including water) can be detrimental to the quality of the deposited film. Similarly, Saitou et al. who used propylene glycol as solvent found that small amounts of resid-

[a] *Prof. P. N. Bartlett, Dr. C. Y. Cummings, Prof. W. Levason, Dr. D. Pugh, Prof. G. Reid*
Chemistry, University of Southampton
Highfield, Southampton, SO17 1BJ (UK)
E-mail: g.reid@soton.ac.uk

Supporting information for this article is available on the WWW under http://dx.doi.org/10.1002/chem.201400179.

© 2014 The Authors. Published by Wiley-VCH Verlag GmbH & Co. KGaA. This is an open access article under the terms of the Creative Commons Attribution License, which permits use, distribution and reproduction in any medium, provided the original work is properly cited.

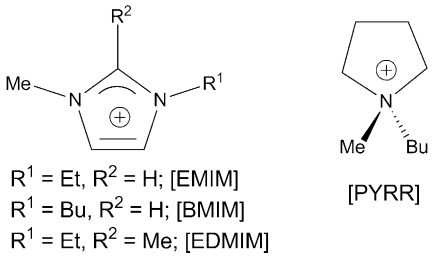

Figure 1. Cations referred to in this work.

ual water were reduced to H_2, which was incorporated into the electrodeposited germanium film.[10]

Recently, we reported the supercritical fluid electrodeposition (SCFED)[11] of germanium films by using $GeCl_4$ in sc-CO_2/MeCN and sc-CH_2F_2 (sc = supercritical), with [N*n*Bu$_4$]Cl as the supporting electrolyte.[12] It seems likely that the chlorometallate complex [N*n*Bu$_4$][$GeCl_5$] was formed in situ in this electrolyte system.[13] The resulting films contained oxide contamination, possibly due to the readily hydrolysed $GeCl_4$ reacting with residual water in the supercritical fluid (scf). In an attempt to probe the factors that govern the redox potentials in germanium complexes, as well as access "second-generation" Ge-containing precursors, which are less sensitive to water, we have examined several well-defined halometallate anions of germanium with counterions, such as imidazolium and pyrrolidinium (Figure 1). The halometallate compounds are generally solids, thus easier to handle than liquid $GeCl_4$, less moisture sensitive owing to being coordinatively saturated at germanium, and should have reduction potentials within the accessible solvent window (cf. Endres' work with RTILs). Additionally, by using well-defined molecular species as precursors, controlling the speciation in solution should be more straightforward, thus reducing the complexity of the overall electrochemical system.

Herein, we report the synthesis of halometallate anions of germanium in both the +4 and +2 oxidation states. All complexes have been characterised by NMR spectroscopy (^{1}H and ^{13}C{^{1}H}), IR spectroscopy, elemental analysis and, in most cases, single-crystal X-ray diffraction. To gain a deeper insight into the factors that influence the electrochemical behaviour of these species, we have explored the effects that systematic changes in the cation, oxidation state at germanium and halide co-ligands have on a) the solid-state interactions between cation and anion; b) the spectroscopy and the cyclic voltammetry of the germanium salts in CH_2Cl_2 solution.

Results and Discussion

Chlorogermanate(IV) dianions: effect of the cation

Other than [GeF_6]$^{2-}$, halometallate anions of Ge^{IV} are rare.[14] In 1940, the inorganic salt Cs_2GeCl_6 was reported, which contained a six-coordinate, octahedral environment at germanium.[15] The next structurally authenticated example, [PPh_4]$_2$[$GeCl_6$], was published only in 1997,[16] although [N*n*Bu$_4$][$GeCl_5$] and [NEt_4]$_2$[$GeCl_6$] were both characterised on the basis of vibrational spectroscopy in the meantime.[13,17] Cowley et al. also observed the five-coordinate trigonal bipyramidal [$GeCl_5$]$^-$ monoanion with amido-stabilised phosphenium and arsenium cations,[18] and we recently synthesised the salt [$GeCl_3(OPMe_3)_3$]$_2$[$GeCl_6$] from the reaction of $GeCl_4$ and $OPMe_3$.[19] The heavier [$GeBr_6$]$^{2-}$ and [GeI_6]$^{2-}$ dianions are not known, even as inorganic salts.

Previous attempts to synthesise the [$GeCl_6$]$^{2-}$ dianion directly used either $SOCl_2$ or a 1:2 mixture of EtOH and 12 N HCl. In our hands, the chlorogermanate dianion was readily prepared by adding a solution of $GeCl_4$ in CH_2Cl_2 to a solution of the ap-

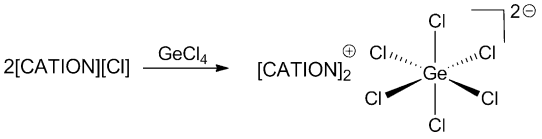

Scheme 1. Synthesis of Ge^{IV} halometallate complexes. [CATION] = [EMIM], [EDMIM] and [PYRR].

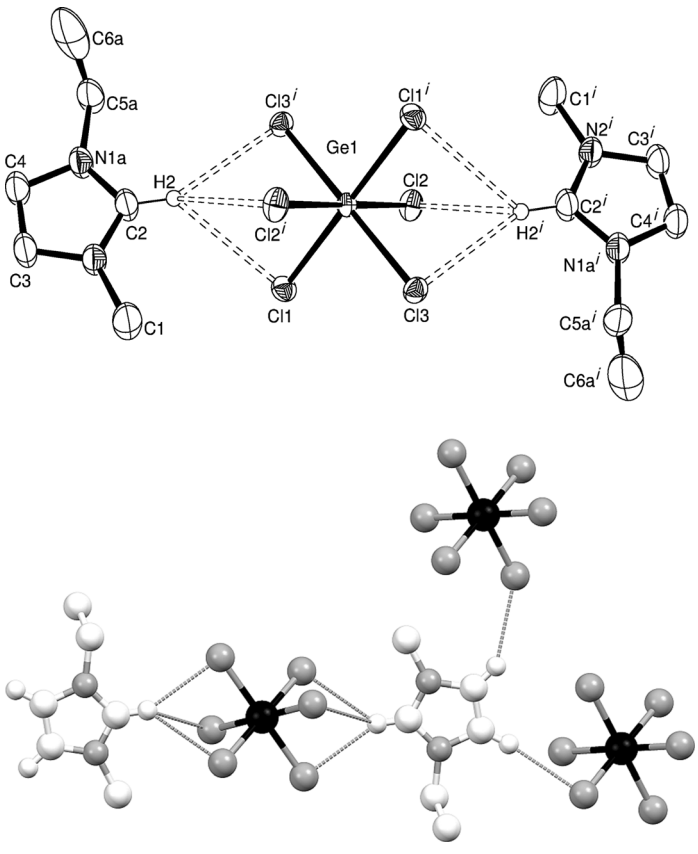

Figure 2. a) ORTEP representation of [EMIM]$_2$[$GeCl_6$] showing hydrogen bonds through H2 as dotted lines. Thermal ellipsoids are drawn at 50% probability. Hydrogen atoms (bar H2), CH_2Cl_2 solvent molecule and disorder of the ethyl group are omitted for clarity. Symmetry code: (i) 2−*x*, −*y*, −*z*. Selected bond lengths [Å]: Ge—Cl1 2.2948(8), Ge—Cl2 2.2855(8), Ge—Cl3 2.3068(9), H2···Cl1 2.9268(9), H2···Cl2 2.9025(9), H2···Cl3 2.7238(8); b) diagram showing a portion of the extended structure of [EMIM]$_2$[$GeCl_6$] (Ge = black; Cl, N = grey; C, H = white spheres).

 © 2014 The Authors. Published by Wiley-VCH Verlag GmbH & Co. KGaA, Weinheim

propriate imidazolium or pyrrolidinium chloride in CH_2Cl_2 at ambient temperature. The ratio of reactants is irrelevant to the speciation of the isolated product, but optimum yields were obtained with a 1:2 ratio of $GeCl_4$ to chloride salt (Scheme 1).

Reaction of $GeCl_4$ with [EMIM]Cl gave a white solid upon removal of all volatiles. The solid is soluble in chlorocarbons, and large colourless crystals were grown through the vapour diffusion of Et_2O into a concentrated CH_2Cl_2 solution. The IR spectrum showed a single strong peak at $\tilde{\nu} = 299\ cm^{-1}$, consistent with previous reports of the $[GeCl_6]^{2-}$ dianion.[13] There is no evidence of splitting of this peak, consistent with the high symmetry at Ge, which was observed crystallographically (Figure 2a).

The structure of $[EMIM]_2[GeCl_6]$ showed the expected homoleptic octahedral coordination environment at germanium. Each $[GeCl_6]^{2-}$ dianion has two associated $[EMIM]^+$ cations, with each cation hydrogen bonding to one "face" of the dianion through the acidic H2 proton. The other protons attached to the imidazolium ring are also involved in hydrogen bonding to neighbouring $[GeCl_6]^{2-}$ dianions, creating a 3D network of interconnected cations and anions with hydrogen bond lengths of approximately 2.73 and 2.81 Å for H4 and H5, respectively (Figure 2b). A notable feature of the hydrogen bonding is that the C2–H2 vector is not aligned with the germanium centre, instead it is slightly offset to one side resulting in one significantly shorter H···Cl hydrogen bond.

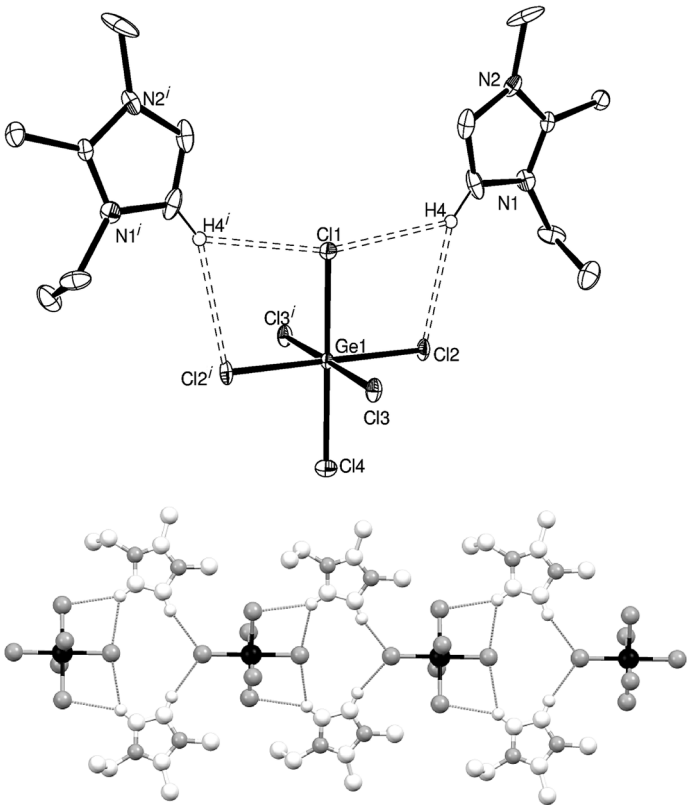

Figure 3. a) ORTEP representation of $[EDMIM]_2[GeCl_6]$. Thermal ellipsoids are drawn at 50% probability, H atoms (bar H4) are omitted for clarity. Symmetry code: (i) $1.5-x$, $1.5-y$, z. Selected bond lengths [Å]: Ge–Cl1 2.303(2), Ge–Cl2 2.312(2), Ge–Cl3 2.276(1), Ge–Cl4 2.301(2), H4···Cl1 2.868(1), H4···Cl2 2.795(2); b) diagram showing the extended structure of $[EDMIM]_2[GeCl_6]$ (Ge = black; Cl, N = grey; C, H = white spheres).

Evidence that some association of the cations is also present in solution comes from the chemical shift of the H2 proton in the ^1H NMR spectrum. For salts, such as $[EMIM][BF_4]$ and $[EMIM][PF_6]$,[20] containing conventional weakly coordinating anions, the resonance associated with the H2 proton is observed at $\delta = 8.55$ and 8.86 ppm, respectively ($CDCl_3$ solution; for details, see the Supporting Information). For [EMIM]Cl, the H2 resonance is observed at 10.47 ppm, significantly to high frequency due to association between H2 and the chloride ion (see the Supporting Information). At $\delta =$ 10.75 ppm, the H2 resonance observed in a $CDCl_3$ solution of $[EMIM]_2[GeCl_6]$ is even further to high frequency, suggesting significant association through H2. The backbone protons H4 and H5 were observed at 7.41 ppm, which is consistent with the reported range of 7.24–7.40 ppm for $[EMIM][BF_4]$ and $[EMIM][PF_6]$.

To analyse the structural effect of removing the acidic proton, H2, the reaction was repeated with 2,3-dimethyl-1-ethyl imidazolium chloride, [EDMIM]Cl. The $[EDMIM]^+$ cation contains a methyl group at the C2 position, thus the most acidic proton H2 is no longer available for hydrogen bonding. The desired product $[EDMIM]_2[GeCl_6]$ was obtained as a white solid, highly soluble in chlorocarbons, and was crystallised through vapour diffusion of Et_2O into a concentrated CH_2Cl_2 solution.

Structural characterisation revealed that the $[GeCl_6]^{2-}$ dianion was stabilised by hydrogen bonds from the two associated $[EDMIM]^+$ cations (Figure 3a). Although $[EDMIM]^+$ does not have the acidic H2 to take part in hydrogen bonding, the backbone protons H4 and H5 are capable of acting as more modest hydrogen-bond donors (as has been seen for $[EMIM]_2[GeCl_6]$ described above). The structural differences between $[EMIM]_2[GeCl_6]$ and $[EDMIM]_2[GeCl_6]$ are notable, with the proton H4 bonding to two chlorides for $[EDMIM]^+$ and only one for $[EMIM]^+$. The other backbone proton, H5, bonds to one chloride acceptor on a neighbouring $[GeCl_6]^{2-}$ dianion [distance H5···Cl4 2.71 Å], which has the effect of creating a ring with two $[GeCl_6]^{2-}$ dianions bridged by two $[EDMIM]^+$ cations. The rings are similar to those observed in the solid-state structure of [EDMIM]Cl, which forms a dimer with two $[EDMIM]^+$ cations bridging between two chlorides through H4 and H5.[21] The difference with $[EDMIM]_2[GeCl_6]$ is that each dianion forms hydrogen bonds to two further $[EDMIM]^+$ cations, creating a 1D chain of orthogonal $[EDMIM]_2[GeCl_6]_2$ rings in the solid state (Figure 3b). The IR spectrum of this salt shows two bands at $\tilde{\nu} = 319$ and 291 cm^{-1}, which we assign to $\tilde{\nu}$(Ge–Cl), consistent with the lower symmetry in the observed structure arising from hydrogen bonding.

In the solution ^1H NMR spectrum of $[EDMIM]_2[GeCl_6]$ ($CDCl_3$), the H4 and H5 protons showed high-frequency shifts to $\delta =$ 7.67 (H4) and 7.57 ppm (H5), each approximately 0.3 ppm from the values observed for $[EMIM][BF_4]$, $[EMIM][PF_6]$ and $[EMIM]_2$-

 © 2014 The Authors. Published by Wiley-VCH Verlag GmbH & Co. KGaA, Weinheim

$[GeCl_6]$; hence, also indicative of some cation association through these H atoms.

If a cation with no acidic protons, such as in [PYRR]Cl, was used, a white solid could be obtained from the reaction with $GeCl_4$. Large colourless crystals were grown through vapour diffusion of Et_2O into a concentrated CH_2Cl_2 solution, but the crystals were exceptionally sensitive to solvent loss, and no viable dataset could be obtained. However, both microanalytical data and IR spectroscopy [$\tilde{\nu}$(Ge–Cl) 301 cm^{-1}] support the presence of a $[GeCl_6]^{2-}$ dianion.

Attempts to form analogous halometallates of germanium(IV) with bromide or iodide were unsuccessful, with the starting materials being recovered in all cases.

Cyclic voltammograms of the Ge^{IV} salts were obtained at a concentration of 5.0 mM in CH_2Cl_2 with 100.0 mM supporting electrolyte and 500 μM of ferrocene (Figure 4 and Table 1). The supporting electrolyte was chosen to be the $[BF_4]^-$ salt of the cation present in the germanium reagent being analysed, that is, [EMIM][BF_4] was the supporting electrolyte for $[EMIM]_2[GeCl_6]$, avoiding the introduction of other strongly coordinating ions into the solution. Cyclic voltammograms of all the supporting electrolytes showed an accessible potential range of approximately −1.0 V to +2.5 V versus Ag|AgCl|0.1 M [N*n*Bu_4]Cl (see the Supporting Information). The ferrocene/ferrocenium redox couple was evaluated to standardise the peak positions of the germanium salts investigated.

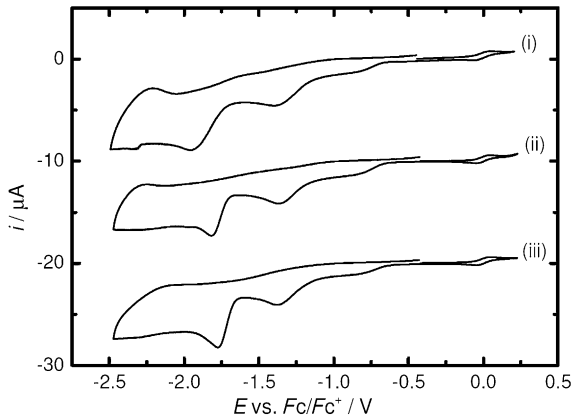

Figure 4. Cyclic voltammograms recorded in CH_2Cl_2 at a 0.5 mm Pt disc working electrode by using a scan rate of 50 mV s^{-1}. The composition of each electrolyte system was: i) 5.0 mM $[EMIM]_2[GeCl_6]$ and 100 mM [EMIM][BF_4]; ii) 5.0 mM $[EDMIM]_2[GeCl_6]$ and 100 mM [EDMIM][BF_4]; and iii) 5.0 mM $[PYRR]_2[GeCl_6]$ and 100 mM [PYRR][BF_4]. Ferrocene (500 μM) was also added to each solution.

Table 1. Summary of electrochemical data for the Ge^{IV} complexes.

Ge^{IV} complex	E_{PC}[a] [V]	I_{PC} [μA]	D[b] [$cm^2 s^{-1}$]
$[EMIM]_2[GeCl_6]$	−1.38	4.55	1.2×10^{-5}
	−1.95		
$[EDMIM]_2[GeCl_6]$	−1.37	4.07	9.5×10^{-6}
	−1.82		
$[PYRR]_2[GeCl_6]$	−1.36	4.15	1.0×10^{-5}
	−1.77		

[a] Versus Fc/Fc^+. [b] Based on the Delahay equation for irreversible waves and measured for the first reduction in each case.

Cyclic voltammograms recorded for the Ge^{IV} complexes each exhibited two reduction waves. The Faradaic components of the voltammograms changed with time, implying that the nature of the electrode is changing. This could be due to a small amount of material being deposited on the electrode surface during the cyclic voltammetry, hence, only the first cycle is presented herein. The first wave is attributed to a two-electron reduction from Ge^{IV} to Ge^{II}, and the second to a two-electron reduction from Ge^{II} to Ge^0. The potential of the former is essentially independent of the cation, whereas a small variation with cation is evident for the latter (Table 1). The irreversible nature of the reduction waves is probably due to liberation of chloride ligands from the germanium during reduction, which diffuse into the bulk solution and hence are not available to reform the $[GeCl_6]^{2-}$ anion upon re-oxidation.

Halogermanate(II) anions: effect of oxidation state

Halometallate anions of Ge^{II} are more common than those of Ge^{IV}, with well-characterised examples of $[GeX_3]^-$ known for X = Cl and Br.[22] Inorganic salts containing the $[GeI_3]^-$ anion are known, although for $MGeI_3$ (M = K, Rb, Cs, NH_4), the characterisation data are mostly limited to powder X-ray diffraction.[23] $TlGeI_3$ and [P*H*$t$$Bu_3$][$GeI_3$] are the only examples characterised by single-crystal X-ray diffraction.[24]

The compound [EMIM][$GeCl_3$] was synthesised in a similar manner to the Ge^{IV} analogues; [$GeCl_2$(dioxane)] replaced $GeCl_4$ and a 1:1 ratio of [EMIM]Cl/Ge provided optimal yields (Scheme 2).

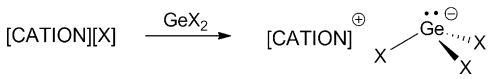

Scheme 2. Synthesis of Ge^{II} halometallate complexes. [X] = Cl: [CATION] = [EMIM], [PYRR], "GeX_2" = [$GeCl_2$(1,4-dioxane)]; [X] = Br, I: [CATION] = [EMIM].

After removal of all volatiles, a viscous oil was obtained (which solidified after several months). The IR spectrum of [EMIM][$GeCl_3$] showed two Ge–Cl vibrations at $\tilde{\nu}$ = 321 and 273 cm^{-1}. These compare well with the bands observed for [NMe_4][$GeCl_3$] ($\tilde{\nu}$ = 303 and 285 cm^{-1}),[25] consistent with the a_1 and e modes expected for the pyramidal $[GeCl_3]^-$ unit. The ^{1}H NMR spectrum exhibited signals for H2 at 9.08 ppm and H4/H5 at 7.33 ppm, only very slightly to high frequency from [EMIM][BF_4], indicating that there is likely only very weak association between the cation and anion in solution. Confirmation of these weak interactions came from an X-ray crystallographic analysis of the colourless crystals of [EMIM][$GeCl_3$] which formed over several months at ambient temperature (Figure 5 a).

The structure shows that [EMIM][$GeCl_3$] is composed of chains of pyramidal $[GeCl_3]^-$ anions linked through intermolecular Ge···Cl secondary interactions. This results in an overall five-coordinate distorted square-based pyramidal geometry at

 © 2014 The Authors. Published by Wiley-VCH Verlag GmbH & Co. KGaA, Weinheim

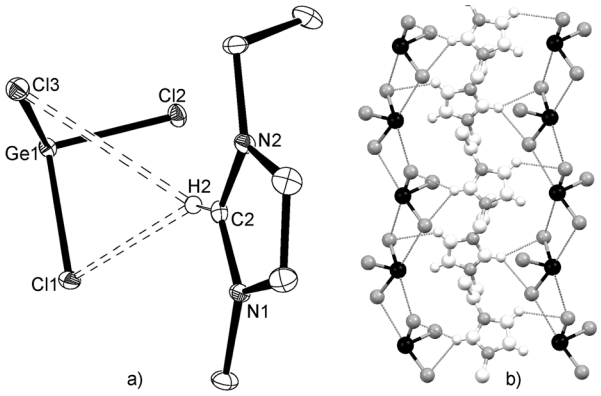

Figure 5. a) ORTEP representation of $[EMIM][GeCl_3]$. Thermal ellipsoids are shown at 50% probability, hydrogen atoms (bar H2) are omitted for clarity. Selected bond lengths [Å]: Ge–Cl1 2.345(1), Ge–Cl2 2.335(1), Ge–Cl3 2.334(1), H2···Cl1 2.828(1), H2···Cl3 2.785(1); b) diagram showing the extended structure of $[EMIM][GeCl_3]$ (Ge = black; Cl, N = grey; C, H = white spheres).

germanium. The Ge···Cl interactions of 3.459(1) and 3.545(1) Å are well within the sum of the van der Waals radii for Ge and Cl (2.29 and 1.82 Å, respectively),[26] but are approximately 1.2 Å longer than the primary Ge–Cl bonds. Two columns of $[EMIM]^+$ cations with alternating arrangements of Et groups cross-link the chains, with the cations hydrogen bonding through H2 and H4 to chlorides [H4···Cl 2.91 Å]. There are no bonds associated with the other backbone proton H5 (Figure 5b). The hydrogen bonds are slightly longer than comparable bonds in $[EMIM]_2[GeCl_6]$, indicating that they are weaker for Ge^{II} chlorometallates than for Ge^{IV}.

A colourless oil formed when [PYRR]Cl was combined with $[GeCl_2$(1,4-dioxane)]. Although the oil did not solidify even when stored at −18 °C, the ^{1}H NMR spectrum was consistent with the pyrrolidinium cation, and the IR spectrum contained two absorptions at $\tilde{\nu}$ = 328 and 279 cm^{-1}, similar to those in $[EMIM][GeCl_3]$ and broadly comparable to $[NMe_4][GeCl_3]$. Elemental analysis also supported the formulation of $[PYRR][GeCl_3]$.

Cyclic voltammograms for the $[GeCl_3]^-$ salts (Figure 6) contained a single reduction wave, assigned as a two-electron reduction from Ge^{II} to Ge^0. The cathodic peak potential (E_{PC}) values for the $[GeCl_3]^-$ salts are approximately midway between those of the first and second reduction waves of the corresponding $[GeCl_6]^{2-}$ salt, indicating that reduction of the $[GeCl_3]^-$ precursors occurs more easily.

Halogermanate(II) anions: effect of the halide

Although Ge^{IV} anions with heavy halogens (Br, I) cannot be formed,[27] heavier halogermanates of Ge^{II} are known. Thus, cyclic voltammetry studies on $[GeX_3]^-$ anions (X = Cl, Br, I) would show the effect of varying the halide co-ligand on the reduction potential. Similar effects have been investigated in transition-metal complexes, for example, reported by Champness et al. with Ru and Os compounds,[28] and by Heath and Sharp with 4d/5d transition metals.[29] To the best of our knowledge, no studies of this nature have been carried out on complexes of p-block elements.

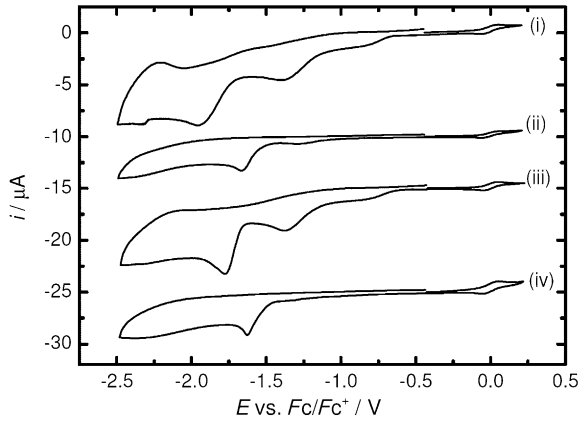

Figure 6. Comparative cyclic voltammograms recorded in CH_2Cl_2 at a 0.5 mm Pt disc working electrode by using a scan rate of 50 $mV\,s^{-1}$. The composition of each electrolyte system was: i) 5.0 mM $[EMIM]_2[GeCl_6]$ and 100 mM $[EMIM][BF_4]$; ii) 5.0 mM $[EMIM][GeCl_3]$ and 100 mM $[EMIM][BF_4]$; iii) 5.0 mM $[PYRR]_2[GeCl_6]$ and 100 mM $[PYRR][BF_4]$; and iv) 5.0 mM $[PYRR][GeCl_3]$ and 100 mM $[PYRR][BF_4]$. Ferrocene (500 μM) was also added to each solution.

Compound $[EMIM][GeBr_3]$ was synthesised by reacting [EMIM]Br with a suspension of $GeBr_2$ in CH_2Cl_2. After removal of all volatiles, a colourless oil, which solidified upon cooling to −18 °C, was isolated. The ^{1}H NMR spectrum of $[EMIM][GeBr_3]$ contained a resonance for H2 at δ = 9.21 ppm, approximately 1.1 ppm to low frequency from [EMIM]Br (10.31 ppm in $CDCl_3$, see the Supporting Information). This is consistent with $[EMIM][GeCl_3]$, which showed very weak interactions between cation and anion in solution. Protons H4 and H5 were observed at 7.39 ppm for $[EMIM][GeBr_3]$ and at 7.57 ppm for [EMIM]Br, again indicative of weaker association for the halometallate salt than the halide salt. One Ge–Br absorption was observed above the cut-off for the IR spectrometer (CsI optics), at $\tilde{\nu}$ = 214 cm^{-1}, consistent with previously reported values for $[GeBr_3]^-$ (i.e., the second peak is expected to occur below 200 cm^{-1}).[22c] Although the majority of the bulk solid was finely powdered, a few colourless crystals, which were suitable for single-crystal X-ray diffraction, were obtained (Figure 7a).

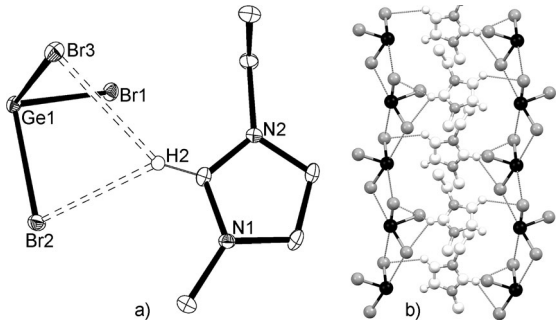

Figure 7. a) ORTEP representation of $[EMIM][GeBr_3]$. Thermal ellipsoids are shown at 50% probability, hydrogen atoms (bar H2) are omitted for clarity. Selected bond lengths [Å]: Ge–Br1 2.4871(7), Ge–Br2 2.5030(7), Ge–Br3 2.5126(7), H2···Br2 2.9626(6), H2···Br3 2.9565(7); b) diagram showing the extended structure of $[EMIM][GeBr_3]$ (Ge = black; Br, N = grey; C, H = white spheres).

 © 2014 The Authors. Published by Wiley-VCH Verlag GmbH & Co. KGaA, Weinheim

Compound [EMIM][$GeBr_3$] is both isomorphous and isostructural with the chloride analogue. The primary coordination environment at germanium is pyramidal, with secondary Ge···Br interactions of 3.4609(8) and 3.5438(9) Å, linking the anions into columns. These interactions are well within the sum of the van der Waals radii for germanium and bromine (2.29 and 1.86 Å, respectively),[26] bringing the overall coordination number at germanium to five with a distorted square-based pyramidal geometry. The $[EMIM]^+$ cation is involved in hydrogen bonds through H2 and H4 (but not H5), with an H4···Br3 distance of approximately 3.01 Å. Two columns of $[EMIM]^+$ cross-link chains of $[GeBr_3]^-$ anions in the solid state are shown in Figure 7b.

The synthesis of [EMIM][GeI_3] was accomplished in a similar manner from [EMIM]I and GeI_2. A dark red solid, which was recrystallised by cooling a saturated CH_2Cl_2 solution to −18 °C, was isolated. Elemental analysis supported the formation of [EMIM][GeI_3]. Further corroboration came from analysis of the ^{1}H NMR spectrum, in which the signal associated with the acidic H2 was located at $\delta = 9.13$ ppm, significantly to low frequency from free [EMIM]I at 9.99 ppm ($CDCl_3$). The backbone H4/H5 protons are also shifted to low frequency from 7.53 ppm in [EMIM]I to 7.39 ppm in [EMIM][GeI_3], confirming that only very weak interactions were retained in solution. Structural characterisation of the crystals was carried out (Figure 8a).

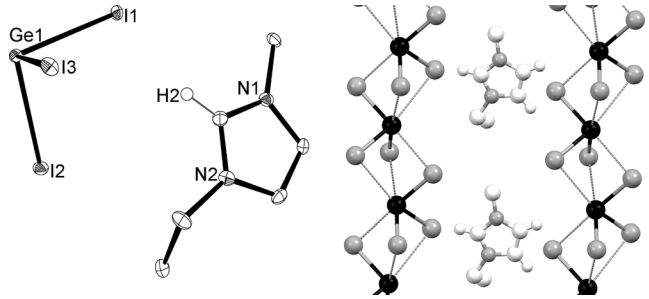

Figure 8. a) ORTEP representation of [EMIM][GeI_3]. Thermal ellipsoids are shown at 50% probability, hydrogen atoms (bar H2) are omitted for clarity. Selected bond lengths [Å]: Ge–I1 2.7873(5), Ge–I2 2.7432(5), Ge–I3 2.7946(5); b) diagram showing the extended structure of [EMIM][GeI_3] (Ge=black; I, N=grey; C, H=white spheres).

[EMIM][GeI_3] crystallises in a different space group to the chloride and bromide analogues (orthorhombic $P2_12_12_1$ vs. monoclinic $P2_1/n$). The primary coordination sphere of germanium is still pyramidal for $[GeI_3]^-$, but the secondary interactions to neighbouring iodides result in an overall six-coordinate distorted octahedron at germanium (Figure 8b). This is different to corresponding $[GeCl_3]^-$ and $[GeBr_3]^-$ salts, which have overall five-coordinate distorted square-based pyramidal geometry. The Ge–I interactions of 3.4180(5), 3.4436(6) and 3.6969(5) Å are all well within the sum of van der Waals radii for Ge and I (2.29 and 2.04 Å respectively), but there is only one H···I distance of approximately 3.20 Å (through H4, not H2), which is less than the sum of van der Waals radii for Ge and H (2.29 and 1.20 Å, respectively).[28] Thus, the $[GeI_3]^-$ units form chains in the solid state, with the $[EMIM]^+$ cations lying between them. This contrasts with the lighter $[GeX_3]^-$ structures (X=Cl, Br), in which a combination of hydrogen bonding between cation and anion and interactions between neighbouring $[GeX_3]^-$ anions were observed in the solid-state structures.

Cyclic voltammograms recorded for [EMIM][GeX_3] (X=Cl, Br, I) all showed a single-reduction wave assigned to Ge^{II} to Ge^0 (Figure 9). When X changes Cl→Br→I, the reduction potential becomes significantly more positive, such that $\Delta E_{PC} = +0.35$ V from [EMIM][$GeCl_3$] to [EMIM][GeI_3], consistent with reduction of the $[GeI_3]^-$ anion being more accessible (Table 2). For $[GeI_3]^-$, additional oxidation features are seen at approximately −0.4 V versus Fc/Fc^+, which correspond to iodide/iodine redox couples from small quantities of free iodide present in the electrolyte.

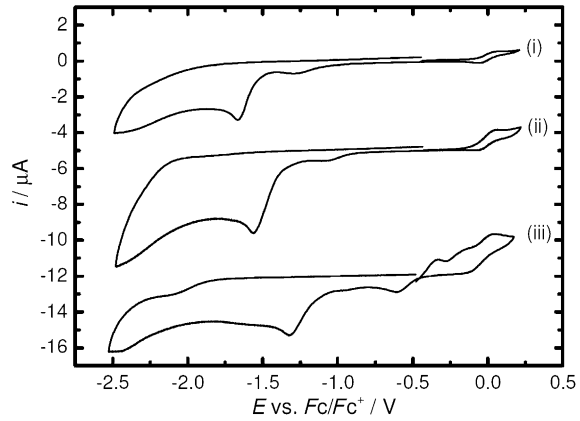

Figure 9. Cyclic voltammograms recorded in CH_2Cl_2 at a 0.5 mm Pt disc working electrode by using a scan rate of 50 mV s^{-1}. The composition of each electrolyte system was: i) 5.0 mM [EMIM][$GeCl_3$] and 100 mM [EMIM][BF_4]; ii) 5.0 mM [EMIM][$GeBr_3$] and 100 mM [EMIM][BF_4]; and iii) 5.0 mM [EMIM][GeI_3] and 100 mM [EMIM][BF_4]. Ferrocene (500 μM) was also added to each solution.

Table 2. Summary of electrochemical data for the Ge^{II} complexes.

Ge^{II} precursor	E_{PC}[a] [V]	I_{PC} [μA]	D[b] [cm^2 s^{-1}]
[PYRR][$GeCl_3$]	−1.63	4.14	9.9×10^{-6}
[EMIM][$GeCl_3$]	−1.67	3.29	6.5×10^{-6}
[EMIM][$GeBr_3$]	−1.56	4.60	1.0×10^{-5}
[EMIM][GeI_3]	−1.32	3.30	6.4×10^{-6}

[a] Versus Fc/Fc^+. [b] Based on the Delahay equation for irreversible waves.

Conclusion

Cyclic voltammograms of seven new halometallate salts of Ge^{IV} and Ge^{II} revealed the effects of changing the cation, oxidation state and halide co-ligand on the reduction potential required to reach the Ge^0 oxidation state. Cations that possess acidic

 © 2014 The Authors. Published by Wiley-VCH Verlag GmbH & Co. KGaA, Weinheim

protons are capable of undergoing significant hydrogen bonding to the halogermanate anion in the solid state, and NMR evidence suggests the cations are associated in solution, albeit more strongly in the Ge^{IV} than Ge^{II} systems. Reduction from the $[GeCl_3]^-$ salts is more accessible than from the $[GeCl_6]^{2-}$ species, and within the $[GeX_3]^-$ species changing the halide co-ligand has a significant effect on the reduction potential to Ge^0, with reduction of [EMIM][GeI_3] occurring 0.35 V more positive compared to [EMIM][$GeCl_3$]. These observations indicate that the speciation of halogermanates in solution is very dependent on the particular cation/anion combinations, and this is also highly likely to be relevant in ionic liquids, and also influence the electrochemical behaviour in these media.

The information gained from this study suggests that an excellent Ge-containing precursor for electrodeposition would be one, which contains 1) a non-coordinating cation, such as $[NnBu_4]^+$ or $[PYRR]^+$; 2) Ge in the +2 oxidation state; and 3) iodide as co-ligand. Further studies are underway to explore the use of such precursors in electrodeposition processes and the results will be reported in due course.

Experimental Section

All preparations were carried out under a dry dinitrogen atmosphere by using standard Schlenk and glove-box techniques. $GeCl_4$, $GeBr_4$, [$GeCl_2$(dioxane)], $GeBr_2$ and GeI_2 were obtained from Sigma, GeI_4 was obtained from Strem, and all were used as received. The ionic liquids were obtained from Sigma and dried by heating under vacuum at 100 °C for 4 h, then stored in a glove box (see the Supporting Information for characterisation data). CH_2Cl_2 was dried by distillation from CaH_2 and Et_2O distilled from sodium benzophenone ketyl.

Infrared spectra were recorded neat (oils) or as Nujol mulls (solids) between CsI plates by using a Perkin–Elmer Spectrum 100 spectrometer over the range 4000–200 cm^{-1}. ^1H and $^{13}C\{^1H\}$ NMR spectra were recorded in $CDCl_3$ or CD_2Cl_2 solutions at 293 K by using Bruker AV-300 and DPX-400 spectrometers and were referenced to the residual solvent resonance. Microanalyses were undertaken by Stephen Boyer at London Metropolitan University.

Electrochemical experiments were carried out within a standard three-electrode cell within a dry, dinitrogen-filled glove box (Belle Technology Limited, UK). The working electrodes used were platinum wires (diameter 0.5 mm) sealed in glass. Electrodes were polished by using Al_2O_3 abrasives from Bunher until a mirror-like finish was attained. The counterelectrode employed was a platinum gauze with the reference being an all CH_2Cl_2 electrode, that is, Ag|AgCl|0.1 M $[NnBu_4]Cl$. Peak potentials were standardised against the observed ferrocene/ferrocenium redox couple. Cyclic voltammetry and chronoamperometry were performed by using a micro III Autolab (Metrohm, Switzerland). The cyclic voltammograms were recorded by starting at the open circuit voltage (−0.5 V vs. Fc/Fc^+) and scanned positive. In all cases, the cyclic voltammogram displayed is from the first cycle.

Synthesis of $[EMIM]_2[GeCl_6]$

A solution of [EMIM]Cl (293 mg, 2.0 mmol) in CH_2Cl_2 (10 mL) was added to a solution of $GeCl_4$ (214 mg, 1.0 mmol) in CH_2Cl_2 (10 mL) and stirred for 16 h. After this time, the solution was concentrated to approximately 5 mL and crystallised through the vapour diffusion of Et_2O into the CH_2Cl_2 solution. Yield: 481 mg, 95%. ^1H NMR (400.1 MHz, CD_2Cl_2): $\delta = 10.75$ (1H, br s, H2), 7.41 (2H, br s, H4/5), 4.35 (2H, q, $J = 6.6$ Hz, CH_2), 4.04 (3H, s, NCH_3), 1.56 ppm (3H, t, $J = 6.8$ Hz, Et CH_3); $^{13}C\{^1H\}$ NMR(100.6 MHz, CD_2Cl_2): 138.97 (CH, C2), 123.80, 122.08 (CH, C4/5), 45.94 (CH_2), 37.24 (NCH_3), 15.96 ppm (Et CH_3); IR (Nujol): $\tilde{\nu} = 299$ cm^{-1} (s; Ge–Cl); elemental analysis calcd (%) for $C_{12}H_{22}Cl_6GeN_4$ (507.54): C 28.37, H 4.37, N 11.04; found: C 28.50, H 4.51, N 11.16.

Synthesis of $[EDMIM]_2[GeCl_6]$

A solution of [EDMIM]Cl (321 mg, 2.0 mmol) in CH_2Cl_2 (10 mL) was added to a solution of $GeCl_4$ (214 mg, 1.0 mmol) in CH_2Cl_2 (10 mL) and stirred for 16 h. After this time, the solution was concentrated to approximately 5 mL and crystallised through the vapour diffusion of Et_2O into the CH_2Cl_2 solution. Yield: 361 mg, 67%. ^1H NMR (400.1 MHz, $CDCl_3$): $\delta = 7.57$ and 7.67 (each 1H, d, $J = 1.8$ Hz, H4/5), 4.19 (2H, q, $J = 7.3$ Hz, CH_2), 3.88 (3H, s, NCH_3), 2.69 (3H, s, C2 CH_3), 1.34 ppm (3H, t, $J = 7.3$ Hz, Et CH_3); $^{13}C\{^1H\}$ NMR (100.6 MHz, $CDCl_3$): $\delta = 143.06$ (C, C2), 122.87 and 120.54 (CH, C4/5), 43.64 (CH_2), 35.48 (NCH_3), 14.97 (Et CH_3), 10.06 (C2 CH_3) ppm; IR (Nujol): $\tilde{\nu} = 319$ (m), 291 cm^{-1} (s; Ge–Cl); elemental analysis calcd (%) for $C_{14}H_{26}Cl_6GeN_4$ (535.57): C 31.39, H 4.89, N 10.46; found: C 31.53, H 5.11, N 10.41.

Synthesis of $[PYRR]_2[GeCl_6]$

A solution of [PYRR]Cl (355 mg, 2.0 mmol) in CH_2Cl_2 (10 mL) was added to a solution of $GeCl_4$ (213 mg, 1.0 mmol) in CH_2Cl_2 (10 mL) and stirred for 16 h. After this time, the solution was concentrated to approximately 5 mL, and Et_2O (40 mL) was added. The white solid was isolated by filtration and dried in vacuo. Crystals highly sensitive to solvent loss were obtained through the slow diffusion of Et_2O into a concentrated CH_2Cl_2 solution. Yield: 419 mg, 74%. ^1H NMR (300.1 MHz, CD_2Cl_2): $\delta = 3.61$–3.80 (4H, m, pyrrolidine NCH_2), 3.50–3.59 (2H, m, butyl NCH_2), 3.19 (3H, s, NCH_3), 2.24 (4H, br s, pyrrolidine NCH_2CH_2), 1.67–1.81 (2H, m, butyl NCH_2CH_2), 1.41 (2H, dq, $J = 7.5$, 14.9 Hz, butyl CH_2CH_3), 0.97 ppm (3H, t, $J = 7.3$ Hz, butyl CH_3); $^{13}C\{^1H\}$ NMR (75.4 MHz, CD_2Cl_2): $\delta = 64.87$ (pyrrolidine NCH_2), 64.53 (butyl NCH_2), 48.99 (NCH_3), 26.35 (butyl NCH_2CH_2), 22.13 (pyrrolidine NCH_2CH_2), 20.29 (CH_2, butyl CH_2CH_3), 13.96 ppm (butyl CH_3); IR (Nujol): $\tilde{\nu} = 301$ cm^{-1} (s; Ge–Cl); elemental analysis calcd (%) for $C_{18}H_{40}Cl_6GeN_2$ (569.68): C 37.94, H 7.07, N 4.92; found: C 38.06, H 7.20, N 5.04.

Synthesis of $[EMIM][GeCl_3]$

[EMIM]Cl (147 mg, 1.0 mmol) was added to a solution of [$GeCl_2$(1,4-dioxane)] (232 mg, 1.0 mmol) in CH_2Cl_2 (20 mL). The [EMIM]Cl slowly dissolved over approximately 15 min, forming a pale violet solution, which was stirred for 16 h. After this time, all volatiles were removed in vacuo, affording a pale violet oil, which crystallised upon standing for several weeks. Yield: 276 mg, 95%. ^1H NMR (400.1 MHz, CD_2Cl_2): $\delta = 9.08$ (1H, s, H2), 7.33 (2H, d, $J = 8.1$ Hz, H4/5), 4.34 (2H, q, $J = 7.1$ Hz, CH_2), 4.02 (3H, s, NCH_3), 1.57 ppm (3H, t, $J = 7.3$ Hz, Et CH_3); $^{13}C\{^1H\}$ NMR(100.6 MHz, CD_2Cl_2): $\delta = 136.59$ (CH, C2), 124.18 and 122.36 (CH, C4/5), 46.17 (CH_2), 37.68 (NCH_3), 15.84 ppm (Et CH_3); IR (neat): $\tilde{\nu} = 321$ (m), 273 cm^{-1} (s, br; Ge–Cl); elemental analysis calcd (%) for $C_6H_{11}Cl_3GeN_2$ (290.09): C 24.84, H 3.82, N 9.65; found: C 24.54, H 3.79, N 9.35.

Synthesis of $[PYRR][GeCl_3]$

A solution of [PYRR]Cl (177 mg, 1.0 mmol) in CH_2Cl_2 (10 mL) was added to a solution of [$GeCl_2$(1,4-dioxane)] (232 mg, 1.0 mmol) in

 © 2014 The Authors. Published by Wiley-VCH Verlag GmbH & Co. KGaA, Weinheim

CH_2Cl_2 (10 mL) and stirred for 16 h. After this time, the solution was filtered, and all solvents were removed, affording a colourless oil. Yield: 274 mg, 85%. ^{1}H NMR (400.1 MHz, CD_2Cl_2): $\delta = 3.52–3.61$ (4H, m, pyrrolidine NCH_2), 3.34–3.40 (2H, m, butyl NCH_2), 3.10 (3H, s, NCH_3), 2.28 (4H, br s, pyrrolidine NCH_2CH_2), 1.72–1.82 (2H, m, butyl NCH_2CH_2), 1.43 (2H, dq, $J = 7.4$, 7.4 Hz, butyl CH_2CH_3), 0.98 ppm (3H, t, $J = 7.4$ Hz, butyl CH_3); ^{13}C{^{1}H} NMR (100.6 MHz, CD_2Cl_2): $\delta = 65.49$ (pyrrolidine NCH_2), 65.27 (butyl NCH_2), 49.72 (NCH_3), 26.29 (butyl NCH_2CH_2), 22.16 (pyrrolidine NCH_2CH_2), 20.13 (CH_2, butyl CH_2CH_3), 13.86 ppm (butyl CH_3); IR (neat): $\tilde{\nu} = 328$ (m), 279 cm^{-1} (s, br; Ge–Cl); elemental analysis calcd (%) for $C_9H_{20}Cl_3GeN$ (321.16): C 33.63, H 6.28, N 4.36; found: C 33.70, H 6.32, N 4.44.

Synthesis of [EMIM][GeBr$_3$]

[EMIM]Br (382 mg, 2.0 mmol) was added to a suspension of $GeBr_2$ (463 mg, 2.0 mmol) in CH_2Cl_2 (20 mL). The $GeBr_2$ dissolved over approximately 15 min, forming a colourless solution, which was stirred for 16 h. After this time, the solution was filtered, and all volatiles were removed in vacuo, affording a colourless oil, which solidified upon cooling to −18 °C with concomitant formation of a few small crystals. Yield: 724 mg, 85%. ^{1}H NMR (300.1 MHz, CD_2Cl_2): $\delta = 9.21$ (1H, s, H2), 7.39 (2H, dt, $J = 5.6$, 1.8 Hz, H4/5), 4.35 (2H, q, $J = 7.3$ Hz, CH_2), 4.03 (3H, s, NCH_3), 1.57 ppm (3H, t, $J = 7.5$ Hz, Et CH_3); ^{13}C{^{1}H} NMR (75.4 MHz, CD_2Cl_2): $\delta = 136.11$ (CH, C2), 124.17 and 122.39 (CH, C4/5), 46.04 (CH_2), 37.56 (NCH_3), 15.83 ppm (Et CH_3); IR (neat): $\tilde{\nu} = 214$ cm^{-1} (sh; Ge–Br); elemental analysis calcd (%) for $C_6H_{11}Br_3GeN_2$ (423.44): C 17.00, H 2.62, N 6.61; found: C 17.15, H 2.77, N 6.71.

Synthesis of [EMIM][GeI$_3$]

[EMIM]I (476 mg, 2.0 mmol) was added to a suspension of GeI_2 (653 mg, 2.0 mmol) in CH_2Cl_2 (20 mL), forming a dark red brown solution, which was stirred for 16 h. After this time, the solution was filtered, and all volatiles were removed in vacuo, affording a dark brown solid. Yield: 991 mg, 88%. Crystals were obtained upon cooling a saturated CH_2Cl_2 solution to −18 °C. ^{1}H NMR (300.1 MHz, CD_2Cl_2): $\delta = 9.13$ (1H, s, H2), 7.39 (2H, dt, $J = 6.2$, 1.8 Hz, H4/5), 4.36 (2H, q, $J = 7.6$ Hz, CH_2), 4.05 (3H, s, NCH_3), 1.60 ppm (3H, t, $J = 7.5$ Hz, Et CH_3); ^{13}C{^{1}H} NMR (75.4 MHz, CD_2Cl_2): $\delta = 135.45$ (CH, C2), 124.30 and 122.60 (CH, C4/5), 46.18 (CH_2), 37.62 (NCH_3), 15.82 ppm (Et CH_3); elemental analysis calcd (%) for $C_6H_{11}I_3GeN_2$ (564.45): C 12.76, H 1.96, N 4.96; found: C 12.86, H 1.96, N 5.03.

X-ray crystallography

Crystals were obtained as described above. Details of the crystallographic data collection and refinement are given in Table 3. Diffractometer for $[EDMIM]_2[GeCl_6]$ and $[EMIM][GeX_3]$ (X = Cl, Br, I): Rigaku AFC12 goniometer equipped with an enhanced sensitivity (HG) Saturn724+ detector mounted at the window of an FR-E+SuperBright molybdenum-rotating anode generator ($\lambda_1 = 0.71073$ Å) with VHF Varimax optics (70 μm focus); for $[EMIM]_2[GeCl_6]$: Rigaku R-axis Spider including curved Fuji-film image plate and a graphite monochromated sealed tube Mo generator ($\lambda_1 = 0.71073$ Å). Cell determination, data collection, data reduction, cell refinement and absorption correction: CrystalClear-SM Expert 2.0 r7.[30] Structure solution and refinement were routine by using WinGX and software packages within[31] except for $[EMIM]_2[GeCl_6]$, in which positional disorder of the ethyl group was satisfactorily modelled using DFIX restraints. Although Q-peaks corresponding to the location of protons were observed in the Fourier difference map, hydrogen atoms were placed in geometrically assigned positions with C–H distances of 0.95 Å (CH), 0.98 Å (CH_3) or 0.99 Å (CH_2) and refined by using a riding model, with $U_{iso}(H) = 1.2\ U_{eq}(C)$ (CH, CH_2) or $1.5\ U_{eq}(C)$ (CH_3). Mercury[32] and enCIFer[33] were used to prepare material for publication. CCDC 973144 ($[EMIM]_2[GeCl_6]$), 973145 ($[EDMIM]_2[GeCl_6]$), 973146 ($[EMIM][GeCl_3]$), 973147 ($[EMIM][GeBr_3]$) and 973148 ($[EMIM][GeI_3]$) contain the supplementary crystallographic data for this paper. These data can be obtained free of charge from The Cambridge Crystallographic Data Centre via www.ccdc.cam.ac.uk/data_request/cif.

Table 3. Selected crystallographic data for the compounds reported in this paper.

Complex	$[EMIM]_2[GeCl_6]$	$[EDMIM]_2[GeCl_6]$	$[EMIM][GeCl_3]$	$[EMIM][GeBr_3]$	$[EMIM][GeI_3]$
formula	$C_{12}H_{22}Cl_6GeN_4{\cdot}CH_2Cl_2$	$C_{14}H_{26}Cl_6GeN_4$	$C_6H_{11}Cl_3GeN_2$	$C_6H_{11}Br_3GeN_2$	$C_6H_{11}GeI_3N_2$
M [g^{-1}mol^{-1}]	592.55	535.68	290.11	423.49	564.46
T [K]	120(2)	100(2)	100(2)	100(2)	100(2)
crystal system	monoclinic	orthorhombic	monoclinic	monoclinic	orthorhombic
space group (no.)	$P2_1/c$ (14)	$Pccn$ (56)	$P2_1/n$ (14)	$P2_1/n$ (14)	$P2_12_12_1$ (19)
a [Å^{-1}]	8.781(2)	8.891(5)	9.083(5)	9.343(2)	8.232(1)
b [Å^{-1}]	12.8457(4)	14.048(5)	8.829(4)	8.895(2)	10.261(2)
c [Å^{-1}]	12.9455(9)	17.850(5)	13.998(6)	14.553(4)	15.762(3)
β [Å]	110.716(9)	90	95.30(1)	95.116(4)	90
U [Å^3]	1365.8(3)	2229.5(2)	1117.7(9)	1204.6(5)	1331.4(4)
Z	2	4	4	4	4
$\mu Mo_{K\alpha}$ [mm^{-1}]	1.910	2.100	3.410	12.450	9.219
F(000)	596	1088	576	792	1008
total reflections	8367	10071	6438	6604	8234
unique reflections	3117	2547	2559	2743	3051
R_{int}	0.025	0.056	0.046	0.034	0.020
R_1 [$I_o > 2\sigma(I_o)$]	0.042	0.060	0.041	0.038	0.015
R_1 (all data)	0.048	0.082	0.052	0.049	0.016
wR_2 [$I_o > 2\sigma(I_o)$]	0.123	0.119	0.078	0.043	0.023
wR_2 (all data)	0.128	0.126	0.082	0.045	0.023

Acknowledgements

We thank the EPSRC for supporting the SCFED project through a Programme Grant (EP/I033394/1). The SCFED Project (www.scfed.net) is a multidisciplinary collaboration of British Universities investigating the fundamental and applied aspects of supercritical fluids.

Keywords: cyclic voltammetry · germanium · halides · hydrogen bonds · X-ray diffraction

 © 2014 The Authors. Published by Wiley-VCH Verlag GmbH & Co. KGaA, Weinheim

[1] a) B. A. Andersson, *Prog. Photovoltaics* **2000**, *8*, 61 – 76; b) M. L. Lee, E. A. Fitzgerald, M. T. Bulsara, M. T. Currie, A. Lochtefeld, *J. Appl. Phys.* **2005**, *97*, 011101.
[2] Y. Maeda, N. Tsukamoto, Y. Yazawa, Y. Kanemitsu, Y. Masumoto, *Appl. Phys. Lett.* **1991**, *59*, 3168 – 3170.
[3] E. Woelk, D. V. Shenai-Khatkhate, R. L. DiCarlo Jr., A. Amamchyan, M. B. Power, B. Lamare, G. Beaudoin, I. Sagnes, *J. Cryst. Growth* **2006**, *287*, 684 – 687.
[4] A. I. Carim, S. M. Collins, J. M. Foley, S. Maldonado, *J. Am. Chem. Soc.* **2011**, *133*, 13292 – 13295.
[5] X. Liang, Y.-G. Kim, D. K. Gebergziabiher, J. L. Stickney, *Langmuir* **2010**, *26*, 2877 – 2884.
[6] X. Liang, Q. Zhang, M. D. Lay, J. L. Stickney, *J. Am. Chem. Soc.* **2011**, *133*, 8199 – 8204.
[7] a) K. M. Kadish, Q. Y. Xu, J. M. Barbe, J. E. Anderson, E. Wang, R. Guilard, *J. Am. Chem. Soc.* **1987**, *109*, 7705 – 7714; b) K. M. Kadish, Q. Y. Xu, J. M. Barbe, J. E. Anderson, E. Wang, R. Guilard, *Inorg. Chem.* **1988**, *27*, 691 – 696.
[8] a) F. Endres, S. Z. El Abedin, *Chem. Commun.* **2002**, 892 – 893; b) F. Endres, S. Z. El Abedin, *Phys. Chem. Chem. Phys.* **2002**, *4*, 1640 – 1648; c) F. Endres, C. Schrodt, *Phys. Chem. Chem. Phys.* **2000**, *2*, 5517 – 5520.
[9] a) R. Al-Salman, S. Z. El Abedin, F. Endres, *Phys. Chem. Chem. Phys.* **2008**, *10*, 4650 – 4657; b) R. Al-Salman, J. Mallet, M. Molinari, P. Fricoteaux, F. Martineau, M. Troyon, S. Z. El Abedin, F. Endres, *Phys. Chem. Chem. Phys.* **2008**, *10*, 6233 – 6237; c) F. Endres, *Phys. Chem. Chem. Phys.* **2001**, *3*, 3165 – 3174; d) F. Endres, *Electrochem. Solid-State Lett.* **2002**, *5*, C38 – C40; e) F. Endres, S. Z. El Abedin, *Phys. Chem. Chem. Phys.* **2002**, *4*, 1649 – 1657.
[10] M. Saitou, K. Sakae, W. Oshikawa, *Surf. Coat. Technol.* **2003**, *162*, 101 – 105.
[11] J. Ke, W. T. Su, S. M. Howdle, M. W. George, D. Cook, M. Perdjon-Abel, P. N. Bartlett, W. Zhang, F. Cheng, W. Levason, G. Reid, J. Hyde, J. Wilson, D. C. Smith, K. Mallik, P. Sazio, *Proc. Natl. Acad. Sci. USA* **2009**, *106*, 14768 – 14772.
[12] J. Ke, P. N. Bartlett, D. Cook, T. L. Easun, M. W. George, W. Levason, G. Reid, D. Smith, W. T. Su, W. Zhang, *Phys. Chem. Chem. Phys.* **2012**, *14*, 1517 – 1528.
[13] I. R. Beattie, T. Gilson, K. Livingston, V. Fawcett, G. A. Ozin, *J. Chem. Soc. A* **1967**, 712 – 718.
[14] W. Levason, G. Reid, W. Zhang, *Coord. Chem. Rev.* **2011**, *255*, 1319 – 1341.
[15] A. W. Laubengayer, O. B. Billings, A. E. Newkirk, *J. Am. Chem. Soc.* **1940**, *62*, 546 – 548.
[16] H. Gruber, U. Muller, *Z. Kristallogr. New Cryst. Struct.* **1997**, *212*, 497 – 498.
[17] D. M. Adams, J. Chatt, J. M. Davidson, J. Gerratt, *J. Chem. Soc.* **1963**, 2189 – 2194.
[18] C. J. Carmalt, V. Lomeli, B. G. McBurnett, A. H. Cowley, *Chem. Commun.* **1997**, 2095 – 2096.
[19] F. Cheng, M. F. Davis, A. L. Hector, W. Levason, G. Reid, M. Webster, W. Zhang, *Eur. J. Inorg. Chem.* **2007**, 2488 – 2495.
[20] S.-T. Lin, M.-F. Ding, C.-W. Chang, S.-S. Lue, *Tetrahedron* **2004**, *60*, 9441 – 9446.
[21] A. K. Abdul-Sada, S. Al-Juaid, A. M. Greenway, P. B. Hitchcock, M. J. Howells, K. R. Seddon, T. Welton, *Struct. Chem.* **1990**, *1*, 391 – 394.
[22] a) L. Apostolico, M. F. Mahon, K. C. Molloy, R. Binions, C. J. Carmalt, I. P. Parkin, *Dalton Trans.* **2004**, 470 – 475; b) F. Cheng, A. L. Hector, W. Levason, G. Reid, M. Webster, W. Zhang, *Angew. Chem.* **2009**, *121*, 5254 – 5256; *Angew. Chem. Int. Ed.* **2009**, *48*, 5152 – 5154; c) F. Cheng, J. M. Dyke, F. Ferrante, A. L. Hector, W. Levason, G. Reid, M. Webster, W. Zhang, *Dalton Trans.* **2010**, *39*, 847 – 856; d) A. L. Hector, W. Levason, G. Reid, M. Webster, W. Zhang, *Dalton Trans.* **2011**, *40*, 694 – 700.
[23] a) L. Guen, P. Palvadeau, M. Spiesser, M. Tournoux, *Rev. Chim. Miner.* **1982**, *19*, 1 – 10; b) N. Jouini, L. Guen, M. Tournoux, *Rev. Chim. Miner.* **1983**, *20*, 141 – 148.
[24] a) N. Jouini, L. Guen, M. Tournoux, *Ann. Chim. Sci. Mater.* **1982**, *7*, 45 – 51; b) P. G. Jones, F. Ruthe, *Private Communication to the CCDC* **2013**, 926019.
[25] P. S. Poskozim, A. L. Stone, *J. Inorg. Nucl. Chem.* **1970**, *32*, 1391 – 1393.
[26] S. Alvarez, *Dalton Trans.* **2013**, *42*, 8617 – 8636.
[27] L. Pauling, *J. Am. Chem. Soc.* **1927**, *49*, 765 – 790.
[28] a) N. R. Champness, W. Levason, R. A. S. Mould, D. Pletcher, M. Webster, *J. Chem. Soc. Dalton Trans.* **1991**, 2777 – 2783; b) N. R. Champness, W. Levason, D. Pletcher, M. Webster, *J. Chem. Soc. Dalton Trans.* **1992**, 3243 – 3247 and references therein.
[29] a) S. Brownstein, G. A. Heath, A. Sengupta, D. W. A. Sharp, *J. Chem. Soc. Chem. Commun.* **1983**, 669 – 670; b) G. A. Heath, K. A. Moock, D. W. A. Sharp, L. J. Yellowlees, *J. Chem. Soc. Chem. Commun.* **1985**, 1503 – 1505.
[30] Rigaku Corporation, Tokyo, Japan, **2011**.
[31] L. J. Farrugia, *J. Appl. Cryst.* **2012**, *45*, 849 – 854.
[32] C. F. Macrae, P. R. Edgington, P. McCabe, E. Pidcock, G. P. Shields, R. Taylor, M. Towler, J. van de Streek, *J. Appl. Cryst.* **2006**, *39*, 453 – 457.
[33] F. H. Allen, O. Johnson, G. P. Shields, B. R. Smith, M. Towler, *J. Appl. Cryst.* **2004**, *37*, 335 – 338.

Received: January 16, 2014
Published online on March 18, 2014

 © 2014 The Authors. Published by Wiley-VCH Verlag GmbH & Co. KGaA, Weinheim